Chapter 8 Radiation Safety

8. 1 Introduction

8. 1. 1 Design principle

Radiation shielding design of the high intensity proton accelerator facilities has been conducted based on the design values listed in Table 8.1.1. The design values have been specified as a half value of the law in order to ensure the reliable safety design, considering the margin of the shielding calculation. However, the exceptional value of 1/20 of the law has been employed as the effective dose for people living near the site boundary of the facilities. This design value is based on the controlled value employed at nuclear power plants: this value is also employed at SPring-8 and KEK.

For the sake of convenience, a radiation controlled area is classified into three areas: (1) Radiation Controlled Area I, registered radiation workers can enter freely any time; (2) Radiation Controlled Area II, access to this area is limited and permissions and the entering procedures are required; (3) Radiation Controlled Area III, access to this area is in principle forbidden.

Since beam line tunnels are going to be constructed underground, the shielding design value is based on ground water activation and the activation of soils near shielding walls. As the average value of radiation dose along beam line tunnels, i.e. radiation dose due to a line source, 5 mSv/h is adopted in the shielding design and, while, for a point source, 11 mSv/h is allowed under the condition of monitoring ground water activation.

Table 8.1.1 Design value for radiation shielding

Area	Design Value	Japanese Law
Site Boundary	＜50 μSv/y	＜250 μSv/3m
General Area	＜0.25 μSv/h	＜20 μSv/w
Radiation Controlled Area I	＜12.5 μSv/h	＜1 mSv/w
Radiation Controlled Area II	＜10 mSv/h	
Radiation Controlled Area III	＞10 mSv/h	
Ground Water Activation	＜5 mSv/h (11 mSv/h)	

8. 1. 2 Evaluation of radiation and radioactivity

1) Evaluation of radiation

In principle a simple analytical method is used for the evaluation of radiation. Any location, where the simple method cannot be applied (for example, the forward direction of the bulk shielding and a beam dump with the thick interaction region producing radiation), must be evaluated using the detailed calculation method, since the simple method cannot handle such complicated cases.

The shielding design can be summarized as follows:

a) Bulk shielding design: Tesch's equation is used below 1 GeV proton energy and Moyer's model above 1 GeV proton energy: Experimentally determined KEK parameters are employed for the Moyer's model.

b) Duct streaming: the DUCT-III code is used. Accuracy of the code has been examined by various benchmark experiments and the detailed calculations using Monte Carlo simulation. In the case of the detailed evaluation for bulk shielding and duct streaming, Monte Carlo codes: NMTC/JAM, MCNPX, MARS and a two dimensional Sn code, DORT, have been used.

c) Skyshine: the Stapleton's equation has been used; its accuracy has been examined by comparing with Monte Carlo calculations.

Proton energy dependent parameters used for the Moyer's model, the Tesch's equation and the Stapleton's equation are summarized in Table 8.1.2.

The reference density value of the shielding materials we are using in the design calculation are specified as 7.7, 2.2 and 1.5 (g/cm^3) for iron, ordinary concrete and soil, respectively.

Table 8.1.2. Parameters for Moyer's model, Tesch's eq.and Stapleton's eq. used in the design calculation

Proton energy (GeV)	Attenuation length λ (g/cm^2)			Tesch's eq.	Moyer's model	Stapleton's eq.	
	Concrete	soil	iron	H_{casc} [Sv m^2]	H_0 [Sv m^2]	λ (Ec) [m]	g [Sv m^2]
0.06	37	36	49	1.2×10^{-17}	—	320	1.01×10^{-14}
0.2	73	71	135	3.5×10^{-16}	—	438	1.21×10^{-14}
0.4	90	88	136	2.0×10^{-15}	—	502	1.32×10^{-14}
0.45	93	91	139	2.8×10^{-15}	—	510	1.32×10^{-14}
1.5	143	139	188	—	1.32×10^{-13}	600	1.44×10^{-14}
3	143	139	188	—	2.64×10^{-13}	638	1.45×10^{-14}
15	143	139	188	—	1.32×10^{-12}	670	1.47×10^{-14}
50	143	139	188	—	4.40×10^{-12}	670	1.47×10^{-14}

2) Evaluation of radioactivity

The evaluation of radioactivity produced in accelerator components, air inside beam line tunnel and cooling water was based in principle on the measurement at KEK. Since the application of the measurement values to the evaluation is limited, induced activities in accelerator components have been estimated by the detailed calculation using NMTC-MCNP, DCHAIN/SP and QAD. Activities in air and cooling water were estimated using leakage

fluxes of protons and neutrons, which were calculated by NMTC-MCNP, and activation cross sections determined by experiments and the calculation with INC/GEM. Diffusion effect of radioactivity exhausted from stacks to the site boundary was calculated using Pasquil's equation. Radioactivity such as ^{24}Na contained in sludge has been estimated based on the measurements at KEK and LAMPF.

8. 2 Shielding Design for the Linac

8. 2. 1 Beam loss assumption

The beam loss is assumed from the result of particle beam simulation and the measured beam loss at the LAMPF. The assumed beam loss and annual operation time are given in Table 8.2.1.

Table 8.2.1 Assumed beam loss for the Linac

	Power	Energy	Annual operation
	[W]	[MeV]	time [h]
Line Losses			
	1 [nA]	< 100	5500
	0.1 [W/m]	≥ 100	5500
Local Losses			
S62-1	67	62	5500
S72-1	117	72	5500
MEBT2-1	1 [W/m]*5[m]	200	5500
D200-1	108	200	200
MEBT3-1	0.5[W/m]*10[m]	400	5500
L3BT (arc/collimator)	1 [W/m]*147[m]	400	5200
S400-1	200	400	5200
D400-2	600	400	200
D400-3a	600	400	5200
D400-3b	5400	400	200
D400-4a	2000	400	5200
D400-4b	600	400	200
D450-1	600	450	200

8. 2. 2 Bulk shielding calculations

Figure 8.2.1 shows the typical view of the vertical section of the Linac tunnel. The beam line is laid 11.8m under the ground. Given the geometrical conditions of the beam line tunnel, the design calculations were performed to obtain required thickness of the concrete walls for the design criterion of underground water activation of less than 5 mSv/h and for the ground surface dose criterion of 0.25 μSv/h for a general area. In principle, in the bulk shielding calculations, Tesch's equation was used, while for the exceptional cases of the S400-1, D400-2, -3a, -3b, -4a, -4b, and D450-1, where localized radiation sources are apparent, are made bulk shielding calculations with the MCNPX. The required shielding thickness for the Linac is given in Table 8.2.2.

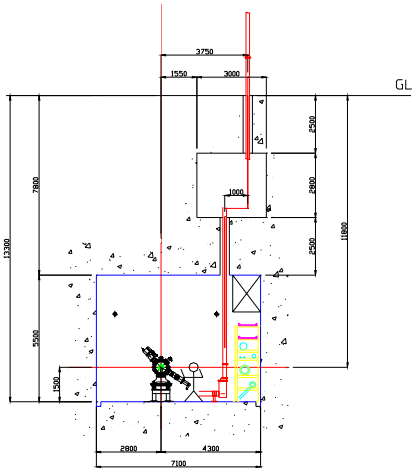

Figure 8.2.1 Typical cross sectional view of the Linac

8. 2. 3 Activation of air in the tunnel

Radioactivity production in air was evaluated using energy fluxes of protons and neutrons in the tunnels, multiplied by the activation cross section data. The energy fluxes were calculated by using the MCNP-X for the cylindrical configuration with the iron target on the axis. Air in the tunnels was assumed to be confined during 20 days operation of the accelerator, and exhausted at several hours after the operation stop.

Figure 8.2.2 shows the concentration of radioactive nuclides in air in the Linac tunnel after 20 days of accelerator operation, where 99% of ^{7}Be is assumed to be removed by a filter. From the figure it is seen that short-lived nuclides ^{13}N and ^{16}N are dominant just after the operation stop, while at several tens hour are left the longer-lived radioactive nuclides such as ^{3}H and ^{14}C. The figure also shows that ^{41}Ar is the most important nuclide at the time of air exhaust, several hours after the operation stop.

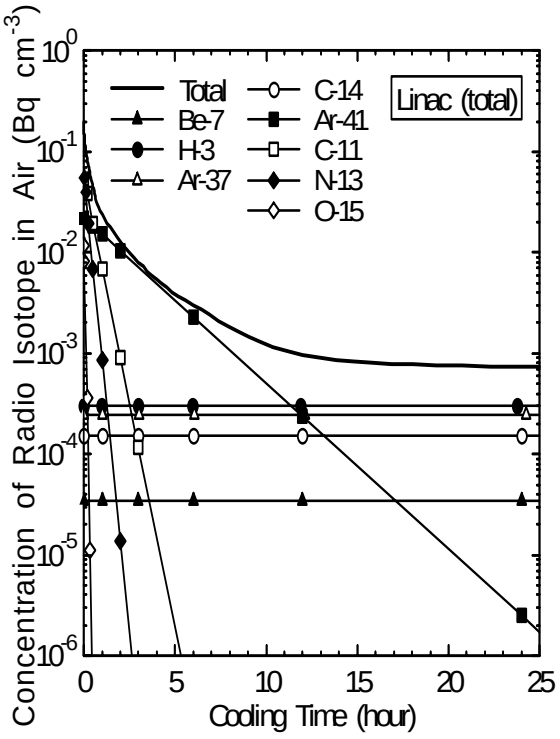

Figure 8.2.2 Concentration of radioactive nuclides in the air

Table 8.2.2 Required shield thickness for the Linac

Position	Tunnel spacing from beam line [cm]				Shielding thickness [cm]								
					top			down		left		right	
	top	bottom	left	right	iron	concrete	soil	iron	concrete	iron	concrete	iron	concrete
60MeV (ion source-SDTL2)	400	150	340	490	0	0	780	0	0	0	0	0	0
S62-1 (next to SDTL-4)	400	150	280	430	0	60	720	0	70	0	60	0	60
S72-1 (next to SDTL-7)	400	150	280	430	0	70	710	0	80	0	70	0	70
200MeV (SDTL3-SDTL32)	400	150	280	430	0	0	780	0	10	0	0	0	0
MEBT2	400	150	280	430	0	40	740	0	60	0	50	0	40
D200-1	400	150	280	430	30	50	730	30	100	30	70	30	50
400MeV (ACS1-ACS46)	400	120	280	430	0	10	770	0	40	0	20	0	10
L3BT straight section	400	120	280	730	0	0	780	0	20	0	0	0	0
MEBT3	400	120	280	430	0	60	720	0	60	0	50	0	40
D400-2	400	120	330	730	100	30	750	100	50	100	30	100	30
D450-1	400	120	630	430	100	30	750	100	50	100	30	100	30
600MeV (SCL1-SCL22)	400	120	280	430	0	10	770	0	50	0	20	0	10
L3BT arc/collimeter section	350	120	260	270	0	70	760	0	120	0	80	0	80
S400-1	350	120	260	270	30	max. 220	-	30	max. 250	30	max.230	30	max.230
Crossing with ADS beam line	350	120	260	270	0	150	680	0	120	0	160	0	80

*The iron is used as local shielding inside the tunnel

8. 2. 4 Activation of the cooling water

Activation of the cooling water was obtained as the product of the energy fluxes of neutrons and protons with the production cross sections of the spallation products.

Annual radioactivity A for the long-lived nuclides is obtained by the following equation;

$$A[\mathrm{Bq/y}] = N_0 \sigma \phi \times \left[1 - \exp\left(-\lambda t_{operation}\right)\right]$$

Here, N_0 is the number of oxygen atoms contained in the cooling water within the components, and $t_{operation}$ the annual operation time of 5500 hours for the Linac.

As for short-lived nuclides, the equilibrium activity A_∞ is obtained by the following equation, considering decay of the nuclides during transportation;

$$A_\infty[\mathrm{Bq \cdot s^{-1}}] = n_0 \sigma \phi \times \exp\left(-\lambda t_{trans.}\right)\left[1 - \exp\left(-\lambda t_{irrad.}\right)\right]\left[1 - \exp\left(-\lambda T\right)\right]^{-1}.$$

Here, n_0 is the number of oxygen atoms contained in the cooling water within the components per unit time: $t_{trans.}$, t_{irrad}, and T are transportation time, irradiation time and circulation-time, respectively.

Annual radioactivity of the long-lived nuclides and that of the short-lived ones are given in Tables 8.2.3 and 8.2.4, respectively.

Table 8.2.3 Annual activities of long-lived nuclides for the Linac [Bq/cm^3]

Nuclide	half-life	unit	Water storage [m^3]				Total activities [Bq/y]
			RI #3	RI #4	RI #5	RI #6	
			28	54	62	7	
H-3	12.33	y	4.71E-01	6.88E-01	1.48E-02	5.92E+00	9.27E+07
Be-7	53.29	d	8.56E-01	1.39E+00	3.54E-02	1.44E+01	2.02E+08
C-14	5730	y	1.68E-04	2.40E-04	5.16E-06	2.13E-03	3.29E+04
Na-22	2.602	y	8.56E-06	1.39E-05	3.54E-07	1.44E-04	2.02E+03
Sc-46 **	83.8	d	3.35E-02	4.89E-02	1.05E-03	4.22E-01	6.59E+06
Mn-54	312.21	d	2.39E-04	3.89E-04	9.90E-06	4.03E-03	5.65E+04
Fe-59	44.6	d	1.73E-05	2.82E-05	7.17E-07	2.92E-04	4.10E+03
Co-56	77.1	d	2.92E-04	4.75E-04	1.21E-05	4.91E-03	6.89E+04
Co-57	271.77	d	2.36E-04	3.84E-04	9.76E-06	3.97E-03	5.58E+04
Co-58	70.8	d	1.48E-03	2.41E-03	6.13E-05	2.50E-02	3.50E+05
Co-60	5.271	y	5.88E-05	9.55E-05	2.43E-06	9.88E-04	1.39E+04
Zn-65	244.1	d	6.64E-06	1.08E-05	2.74E-07	1.12E-04	1.57E+03

＊ Demineralization by ion-exchange resin are not considered.

＊＊ Extrapolating LAMPF measurement

Table 8.2.4 Equilibrium activities of short-lived nuclides for the Linac [Bq/cm^3]

Nuclide	half-life	unit	Water storage [m^3]				Total activities [Bq/y]
			RI #3	RI #4	RI #5	RI #6	
			28	54	62	7	
C-10	19.26	s	1.12E-03	2.18E+00	1.22E-04	1.12E-02	1.18E+08
Be-11	13.8	s	3.70E-04	2.29E-03	3.19E-05	3.77E-03	1.62E+05
C-11	20.4	m	2.23E+00	3.73E+00	6.92E-02	3.21E+01	4.93E+08
N-13	9.96	m	1.08E+00	4.76E+00	3.25E-02	1.48E+01	3.92E+08
O-14	1.177	m	4.50E-02	1.23E-01	1.96E-03	3.82E-01	1.07E+07
C-15	2.449	s	1.04E-08	1.92E-08	6.56E-11	1.46E-06	1.15E+01
O-15	2.03	m	3.89E+00	7.94E+00	1.22E-01	3.57E+01	7.95E+08
N-16	7.13	s	1.48E-02	3.65E-02	8.36E-04	1.96E-01	3.81E+06
Na-24**	14.959	h	3.94E-02	5.98E-02	1.06E-03	5.02E-01	7.91E+06
Mn-52**	5.59	d	3.94E-02	5.98E-02	1.06E-03	5.03E-01	7.92E+06

＊ Demineralization by ion-exchange resin is not considered.

＊＊ Extrapolating LAMPF measurement

8. 3 3-GeV Synchrotron

8. 3. 1 Bulk shield calculations

To estimate the necessary shielding wall thickness for the maximum power of 1 MW (8.3 x 10^{13} per pulse), we assumed the different type of beam losses in the following:

A) 1 kW loss at the injection septum magnet by the L3BT magnet errors and/or the beam blow-up by the space charge force,

B) 4 kW loss at the collimators during the injection stage,

C) 1 W/m loss at 1.5 GeV around the 3 GeV synchrotron ring,

D) 1 kW loss at the extraction septum magnet due to the possible fast beam blowup or errors such as kicker field and closed orbit.

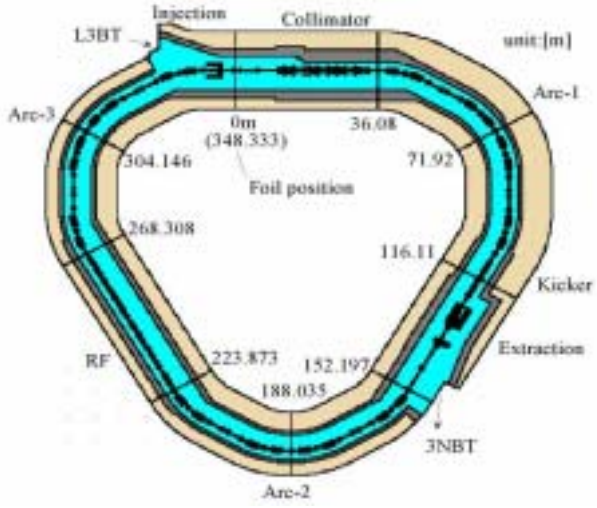

Figure 8.3.1 Overview of whole geometry of 3GeV ring for MARS calculation

For estimation of tunnel shielding thickness of 3-GeV ring, shielding calculations using the simple empirical formula of the Moyer's model and Monte Carlo method were used. In the regions around injection, collimator and extraction where local shields around the beam line are equipped for seriously high beam losses, Monte Carlo calculations using MARS were performed since the Moyer model gives large error in such complicated geometries concerning source term. In other regions where uniform beam loss occurs, Moyer's model was utilized with the parameters mentioned in the Section 8.1. In Fig.8.3.1 is depicted the configuration for MARS calculations.

Figure 8.3.2 shows one of the MARS calculation results for prompt dose equivalent

distributions in the accelerator operation inside the upward concrete and soil shield along the regions from injection through the beginning of the ARC1. The beam loss distribution, which was used in the calculation as source particles, is also shown in the middle of the figure. In the Monte Carlo calculations, only particles of energy higher than 20 MeV are considered. A correction factor from the obtained high-energy dose equivalent to total dose after thick concrete shield is already estimated to be 2.0 by Monte Carlo calculation. Finally, this correction factor and the safety factor 2.0 were multiplied to the MARS calculation results. Based on these shielding calculations, required shield thickness was estimated and tabulated in Table 8.3.1. Shield thickness for the H_0 dump was calculated with NMTC-JAM/MCNP for the design criterion of below 11 mSv/h at the outer concrete boundary. The result is given in Table 8.3.2.

Table 8.3.1 Tunnel inner dimensions and required bulk shield thickness for the 3GeV synchrotron

Tunnel Region			Injection	Collimator	ARC1(connection to collimator)	Kicker	Extraction	RF	ARC	Injection Crane
Range		From [m]	-8.3	10 17.5	38 50	106	119 142	219	70 157 273	329
		To [m]	10	17.5 38	50 70	119	142 157	273	106 219 329	340(-8.3)
Beam loss condition			400 MeV proton 1kW at injection septum 4kW at collimator region			3GeV ptoron 1kW at extraction septum		1.5GeV proton 1W/m uniform		+400MeV 1W/m
Shielding calculation method			Monte Carlo calculation using MARS code					Moyer Model with KEK parameter		
Main Tunnel										
Inner Dimen- sion [cm]	(a)	Upper	320	320	320	320	320	320	320	580
	(b)	Ring inward	550	550	460	470	470	540	460	450
	(c)	Ring outward	400	400 250	240	250	600	240	240	400
	(d)	Lower	120	120	120	120	120	120	120	120
Shield thick- ness [cm]	(e)	Ceiling	270	350	180 120	200	450 250	80	80	220+Iron50
	(f)	Ring inward	220	300	120	150	240 200	30	50	50
	(g)	Ring outward	220	280 330	150	170	220 (3NBT)	100	100	80
	(h)	Floor-Soil	200	220	100	100	300 150	100	100	100
Sub Tunnel										
Inner Dimen- sion[cm]	(i)	Ring inward	550	350	160	150	350 150	160	160	180
	(j)	Ring outward	350	250	240	250	250 250	240	240	220
	(k)	Lower	570	570	570	570	570 570	570	570	570
Shield thick- ness [cm]	(l)	Ceiling	220	220	100	100	220 100	100	100	100
	(m)	Ring inward	100	100	100	100	100 100	20	20	20
	(n)	Ring outward	100	100	100	100	100 100	20	20	20
	(o)	Floor-Soil	130	130	50	130	200 180	50	50	70

Table 8.3.2 Shield thickness of the H_0 dump

Material	Thickness (cm)	
	Lateral	Axis
Graphite	50	100
Iron	150	250
Concrete	300	500

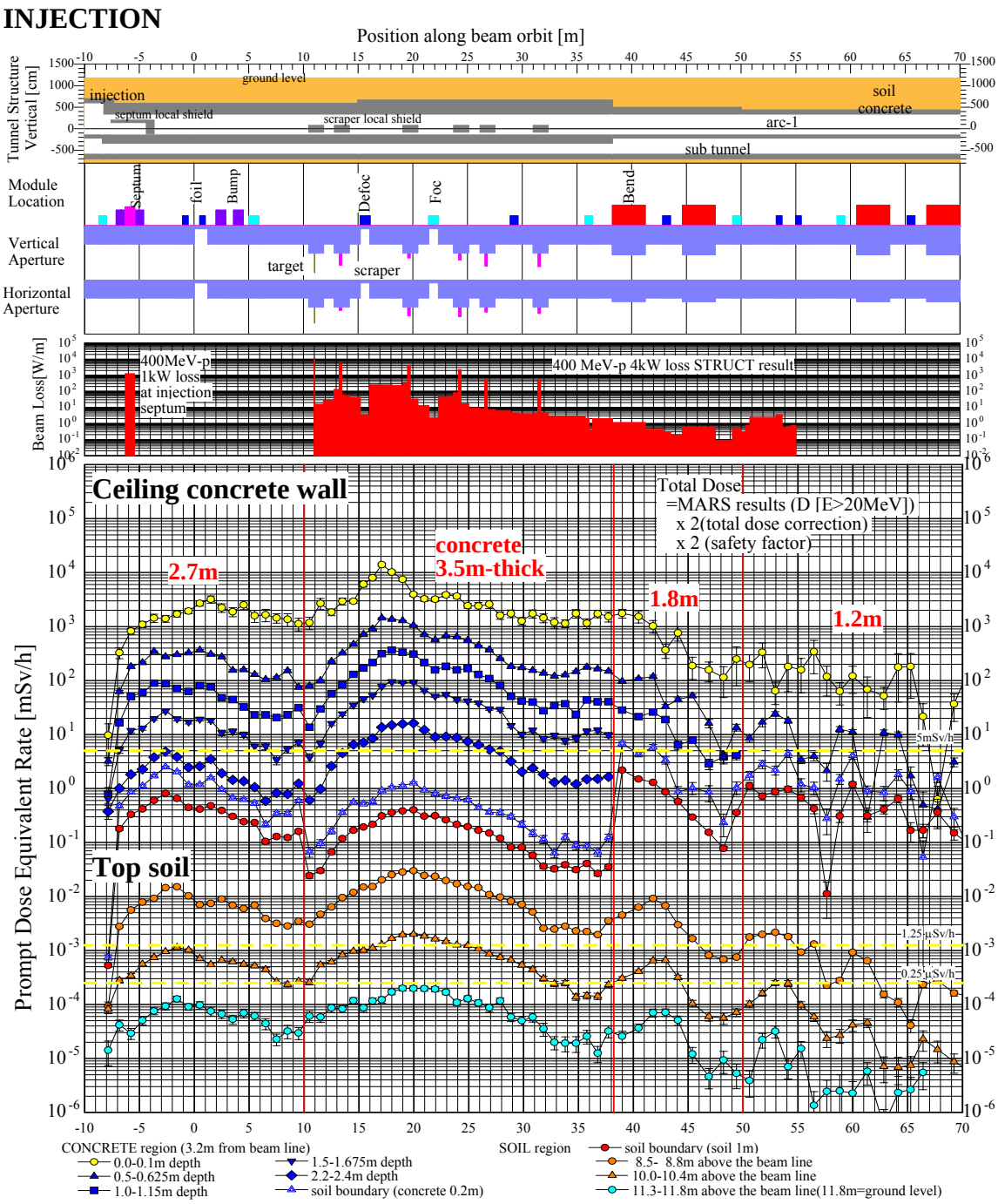

Figure 8.3.2 Prompt dose equivalent distributions inside the ceiling wall and the top soil from injection through ARC. Flux detector locations are shown in Fig.8.3.1. Vertical tunnel structure, module location, vertical and horizontal aperture structures, and beam loss distribution are also shown in the figure.

8. 3. 2 Activation of air and cooling water in the tunnel

Activation of air in the accelerator tunnel was evaluated basically based on the same cross

section data and methods employed for the evaluation for the Linac with an exception for the ventilation condition that air in the tunnel is confined during 20 days operation of the accelerator and is exhausted at several hours after the operation stop.

Figure 8.3.3 shows the concentration of radioactive nuclides in air in the 3 GeV-synchrotron tunnel after 20 days of the accelerator operation, where 99% of ^{7}Be is assumed to be removed by a filter. The decay behavior of the nuclides of interest for the 3-GeV synchrotron is in principle similar to that for the Linac; short-lived nuclides ^{13}N and ^{16}N are dominant just after the operation stop, while at 24 hours after the operation stop are left the longer-lived radioactive nuclides such as ^{3}H and ^{14}C, and ^{41}Ar is the most important nuclide at the time of air exhaust, 10 hours after the operation stop.

Activation of the cooling water is mainly determined by the local loss at the septum magnets in both the injection and extraction regions. Considering only these contribution, preliminary estimation of the annual ^{3}H production was made and the result is given below.

Table 8.3.3 Annual ^{3}H production in the 3-GeV ring cooling water [Bq/y]

	Injection	extraction
^{3}H	3.3×10^{8}	4.1×10^{8}

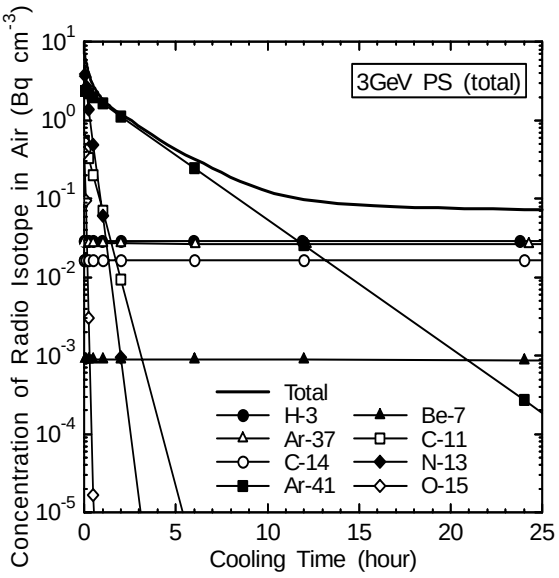

Figure 8.3.3 Concentration of radioactive nuclides in the air for 3-GeV PS ring after 20-days operation of the

8. 4 50-GeV Synchrotron

8. 4. 1 Dose evaluation on the ground surface and the site boundary

In the shielding design, dose rates on the ground level of the beam line tunnels and the evaluation of the dose due to skyshine at the site boundary are important from the point of view of the environmental assessment. Dose rates on the surface of radiation shielding composed of concrete and soils were obtained from the Moyer's model using KEK parameters. In the calculation the beam loss of the 50-GeV synchrotron has been assumed as listed in Table 8.4.1. The skyshine at the site boundary was estimated by the dose rate at the shielding surface of the beam line tunnels. Although dose rates at various beam line tunnels were estimated, a few of typical shielding designs are shown in this report. The cross sectional views of the tunnels at the representative places are shown: Fig.8.4.1, an arc section of the 50-GeV ring; Fig. 8.4.2, a beam

extraction section for the nuclear and particle physics facility; Fig. 8.4.3, a dump structure for the beam injection. Dose rates on the surfaces of shielding are explained in the same figures.

8. 4. 2 Shielding wall design of the 3-50 BT line

The shielding wall has been installed in the transport line in order to ensure the workplace at the downstream, i.e. in the 3-50 BT tunnels and 50-GeV synchrotron ring, even while the 3GeV-synchrotron is operating. Shielding walls and the labyrinthine structure of the side path tunnel in the beam transport tunnel are shown in Fig. 8.4.4 (3-50 BT tunnels and shielding wall) and Fig. 8.4.5 (side path tunnel structure). The shielding wall thickness and the structure of the tunnels were determined by dose rates obtained using the MARS Monte Carlo code. Beam losses were assumed for two cases; 1) an ordinary operation case (3-GeV extraction loss and 3NBT line loss) and 2) an accidental loss of 1 pulse full beam on the beam plugs installed on the beam line axis. The shielding calculation showed a dose rate less than 12.5 μSv/h at the 50 m down stream location in the 3-50 BT beam line tunnel.

8. 4. 3 Further items for the radiation safety design

The following items will be needed to be studied:

1) Cooling water and air activation in the beam line tunnels,

2) Duct-streaming design of the labyrinthine structure for the entrance tunnel,

3) Shielding designs for extraction lines and beam dumps using the MARS code.

Table 8.4.1 Beam Loss in the 50-GeV Synchrotron Ring

injection point	135 W (0.3%)
Synchrotron Quiet Line	0.5 W/m
Extraction Lines	
Slow Extraction Section	7.5 kW (1%)
Fast Extraction Section	1.125 kW (0.15%)
Beam Transfer Line	1 W/m
Dump System	
Injection Line	3 kW (7%)
Extraction Line	7.5 kW(1%)

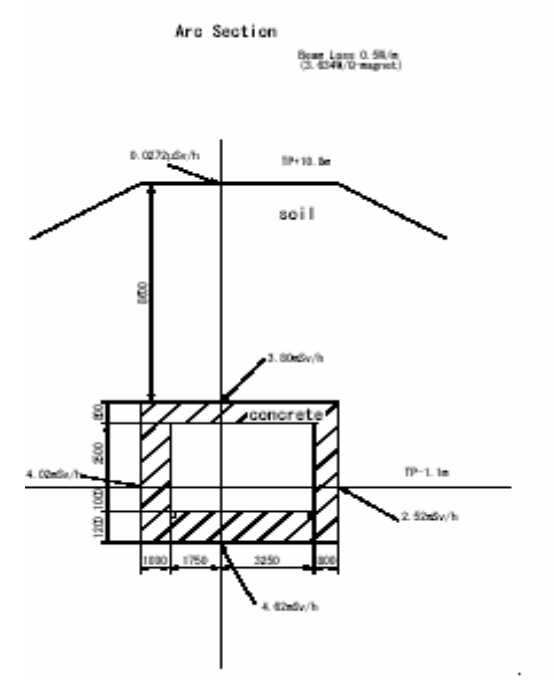

Figure 8.4.1 Arc section in 50-GeV ring. Dose rate on the surface of shielding is 0.027 μSv/h

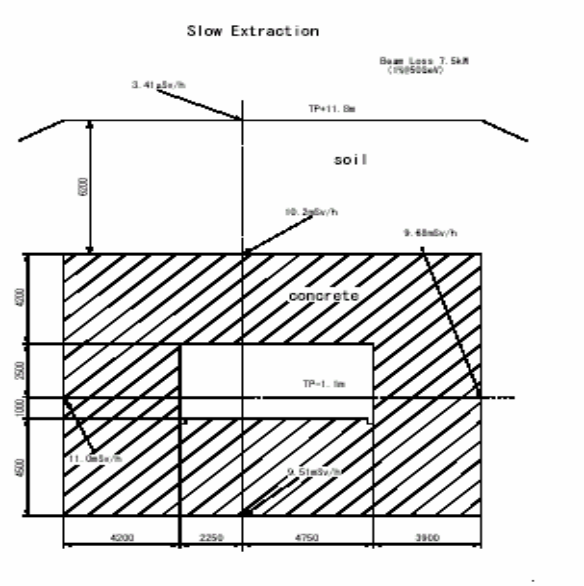

Figure 8.4.2 Slow extraction. Dose rate on the surface of shielding is 3.41 μSv/h (controlled area level)

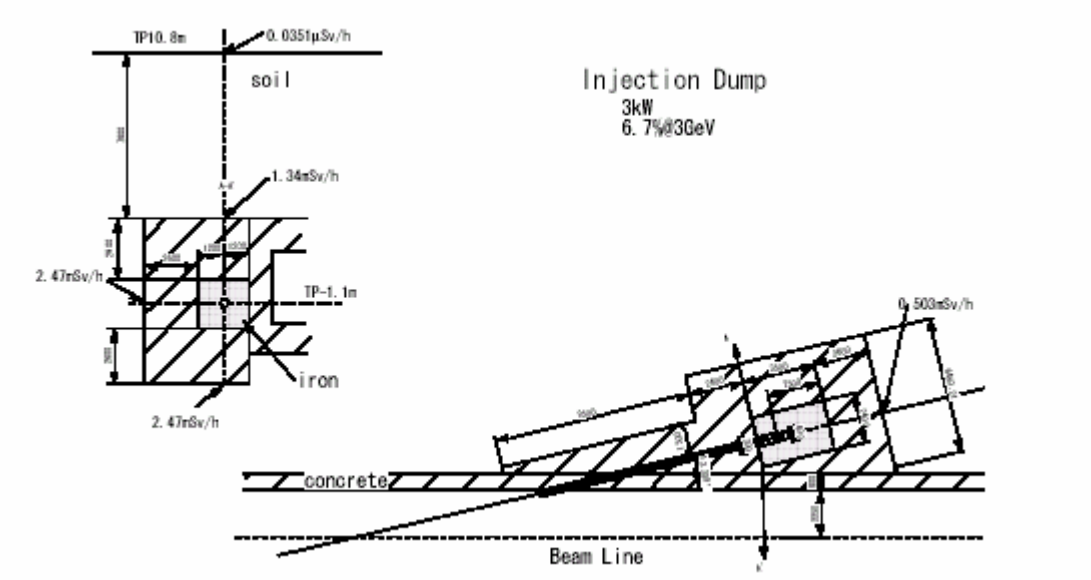

Figure 8.4.3 Injection line dump. Dose rate on the surface of shielding is 0.035 μSv/h

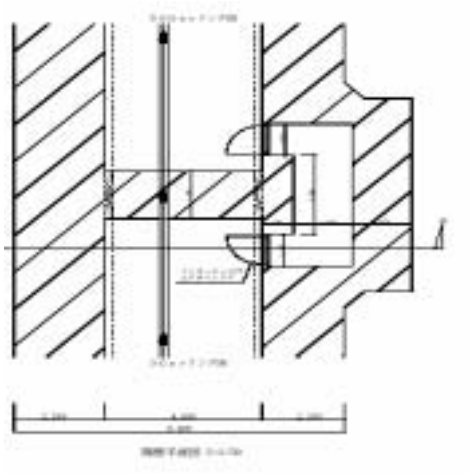

Figure 8.4.4 3 –50 GeV beam transport line and the labyrinthine structure of side path

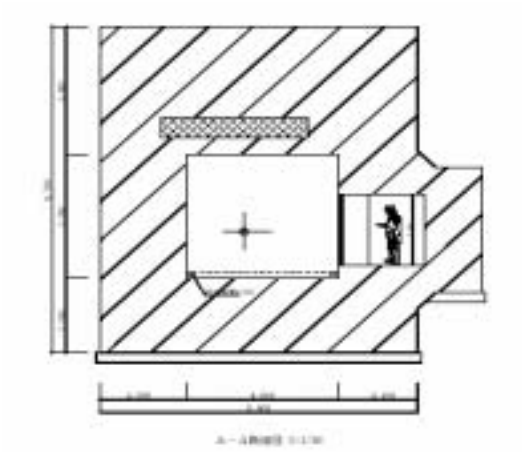

Figure 8.4.5 Cross section of side path

8.5 Proton Beam Line between 3-GeV RCS and Materials and Life Science Facility

The arrangement of the proton beam line between 3-GeV RCS and materials and life science facility is already shown in Fig. 2.2.6.1 of Sec. 2.2.6.1. This beam loss is assumed to be 1 W/m in the proton beam line between 3-GeV RCS and materials and life science facility. Since this beam line has 48 quadrupole and 8 dipole magnets and the length of the beam line is 250 m, the beam loss at each magnet is supposed to be 4.5 W in average. This beam line also has a beam dump of 4 kW, of which shielding design is described in Sec. 3.2.6.5.

The bulk shield of the beam line was mainly designed with the Moyer's model. The typical results are shown in Table 8.5.1. The bulk shield of the switchyard after the extraction of

3-GeV RCS may be affected by the high beam loss (1 kW) in the extraction kicker magnet of 3 GeV. The Monte Carlo calculation with MCNPX is under way.

There exist two pathways in this beam line for cabling and carrying magnets, etc. as shown in Fig. 2.2.6.1 of Sec. 2.2.6.1. The pathways have labyrinth structure for decreasing radiation streaming. Here in Fig.8.5.1, we present as an example a configuration of the labyrinth at the access route to the first utility facility. The shielding performance of the labyrinth structures was estimated by using the MCNPX code. The calculated dose rates at the exit of radiation control area of the first utility facility and the carrying hatch of the second utility facility were around 0.08 and 0.2 μSv/h, respectively. These dose rates are acceptable from the view of radiation safety.

The air and cooling water radioactivity in the beam line (including 4 kW beam dump) from the exit of 3-GeV RCS to the entrance of the materials and life science facility was estimated for beam loss of 1 W/m by using NMTC/JAM, MCNP and DCHAIN-SP. The air and cooling water radioactive concentration is shown in Tables 8.5.2 and 8.5.3 in the case of 20-day operation and cooling of 15 hours, which is less than the discharge regulation limit. The air in the beam line will be released after more than 15 hours of accelerator operation stop. The cooling water will be discharged without dilution every one or two years.

Table 8.5.1 Results of Moyer's model for bulk shield of proton beam line

(a) Under Hakken road

	Upper shield	Lower shield	Right side	Left side
Length from beam line to concrete [m]	3.3	1.2	1.8	2.8
Thickness of concrete [m]	4.5	1.3	1.0	0.7
Dose rate at boundary between concrete and soil [mSv/h]	0.003	4.6	4.8	4.9
Thickness of soil [m]	2.0	-	-	-
Dose rate at ground level [μSv/h]	0.25	-	-	-

(b) Straight part except for Hakken road

	Upper shield	Lower shield	Right side	Left side
Length from beam line to concrete [m]	3.3	1.2	1.8	2.8
Thickness of concrete [m]	0.7	1.3	1.0	0.7
Dose rate at boundary between concrete and soil [mSv/h]	4.5	4.6	4.8	4.9
Thickness of soil [m]	7.8	-	-	-
Dose rate at ground level [μSv/h]	0.11	-	-	-

Table 8.5.2. Radioactivity concentration in air for 20 days operation and cooling of 15 hours

Be-7** (2×10^{-3})*	Ar-37 (7×10^{2})*	H-3 (7×10^{1})*	Ar-41 (5×10^{-4})*	C-14 (2×10^{-2})*
8.0×10^{-6} Bq/cc	2.0×10^{-4} Bq/cc	8.0×10^{-5} Bq/cc	2.0×10^{-4} Bq/cc	3.6×10^{-5} Bq/cc

* : exhaust regulation limit [Bq/cc]

** : after removed by a filter

Table 8.5.3. Radioactivity concentration in water for 20 days operation and cooling of 15 hours

Be-7** (30Bq/cc)*	H-3 (60Bq/cc)*	C-14 (2Bq/cc)*
0.23 Bq/cc	1.25 Bq/cc	0.0035 Bq/cc

* : exhaust regulation limit [Bq/cc]

** : after removed by an ion exchange resin

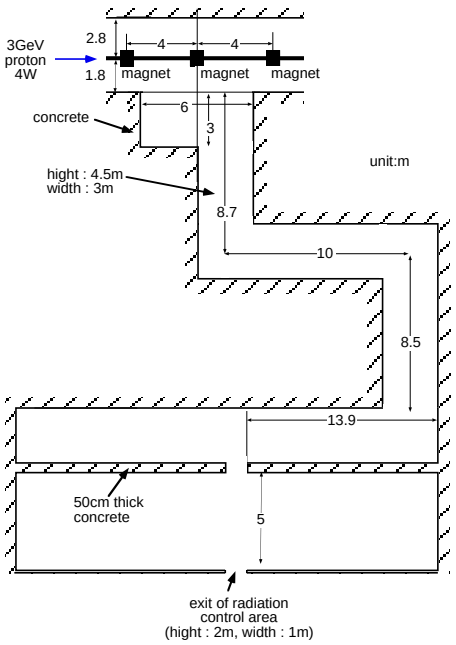

Figure 8.5.1. Access route to the first utility facility

8. 6 Annual Production of Radioactive Gas and Liquid and the Annual Total Exhaust

Radioactive gas, which is exhausted from the facilities in a form of aerosol and gas, is estimated to be about 1.3×10^{12} Bq /y: the main nuclides are ^{3}H, ^{37}Ar, ^{127}Xe, ^{197}Hg, and ^{203}Hg. These gases are exhausted together with an annual total air of about 1.5×10^{9} m^3/y. Radioactive gas in an aerosol form, which is produced by the operation of accelerator facilities, is released after filtering by both pre-filters and high efficiency filters being installed in exhaust systems of each facility. More detailed exhaustion data are given in Table 8.6.1.

Table 8.6.1 Annual exhaust of radioactive gas

(Bq/y)

Nuclide	Linac	3-GeV Synchrotron	Material & Life Science	50-GeV Synchrotron	Nuclear & Particle Physics	Total
^{3}H	5.9×10^{8}	8.3×10^{8}	2.3×10^{11}	1.5×10^{8}	2.3×10^{10}	2.5×10^{11}
^{37}Ar	1.1×10^{8}	2.3×10^{9}	1.7×10^{11}	2.1×10^{9}	—	1.8×10^{11}
^{127}Xe	—	—	2.0×10^{11}	—	—	2.0×10^{11}
^{197}Hg	—	—	2.1×10^{11}	—	—	2.1×10^{11}
^{203}Hg	—	—	2.9×10^{11}	—	—	2.9×10^{11}
total	9.3×10^{8}	5.4×10^{9}	1.2×10^{12}	4.2×10^{9}	2.6×10^{10}	1.3×10^{12}

On the other hand, radioactive liquid exhausted from the facilities is estimated to be 1.3×10^{12} Bq /y: the main nuclide is ^{3}H. The annual water discharge from the facilities is about 1.8×10^{3} m^3 /y. Radioactive water waste exhausted from the facilities is temporarily stored in a tank installed in each facility until the activity decreases below the level allowed for release: then it is released outside facilities through the No. 2 drain. More detailed exhaustion data are given in Table 8.6.2.

Table 8.6.2 Annual exhaust of radioactive liquid

(Bq/y)

Nuclide	Linac	3 GeV Synchrotron	Material & Life Science	50 GeV Synchrotron	Nuclear & Particle Physics	Total
^{3}H	9.9×10^{10}	5.2×10^{9}	8.9×10^{11}	1.7×10^{8}	2.1×10^{11}	1.3×10^{12}

8. 7 Effective Dose due to an Abnormal Incident

A small beam loss of 1 W/m, is assumed for the shielding design except for the specific location in order to work on hands-on-maintenance. Hence, in case of the local unexpected

large beam loss, it is important to evaluate the effect on the radiation safety. In order to estimate the effective dose due to an abnormal incident, the full beam loss of 100% proton beam is assumed to occur at any one point: then the effective doses at the most nearest ground and site boundary are estimated for one pulse of the full beam. The results are shown in Table 8.7.1.

It can be concluded that there is no problem to exceed the allowed effective dose at the site boundary due to one pulse full beam loss. However Table 8.7.1 shows that the most severe case is observed on the ground of the 50 GeV synchrotron facility, where the design condition of the allowed annual-effective dose is 1 mSv/y: considering the frequency of the beam, 1 pulse within about 3 seconds, the full beam loss is allowed about 20 times in a year to satisfy the design level on the ground.

Table 8.7.1 Effective dose due to the 100% beam loss

Facilities	Repetition Frequency	Ground (μ Sv/pulse)	Site Boundary (μ Sv/pulse)
Linac	50	0.042	6.7×10^{-06}
3 GeV－PS	25	0.17	1.3×10^{-05}
3-N BT	25	0.11	6.7×10^{-06}
3-50 BT	25	0.047	3.3×10^{-06}
50 GeV－PS	0.3	49	5.3×10^{-02}
ν －BT	0.3	6.7	1.7×10^{-04}
K－BT	0.3	4.6	1.0×10^{-03}